Numer. Math. Theor. Meth. Appl. Vol. **5**, No. 1, pp. 43-61
doi: 10.4208/nmtma.2011.m12si03 February 2012

An Iterative Multigrid Regularization Method for Toeplitz Discrete Ill-Posed Problems

Marco Donatelli*

Dipartimento di Fisica e Matematica, Università dell'Insubria, Via Valleggio, 11, Como 22100, Italia.

Received 01 December 2010; Accepted (in revised version) 05 May 2011

Available 21 December 2011

Abstract. Iterative regularization multigrid methods have been successful applied to signal/image deblurring problems. When zero-Dirichlet boundary conditions are imposed the deblurring matrix has a Toeplitz structure and it is potentially full. A crucial task of a multilevel strategy is to preserve the Toeplitz structure at the coarse levels which can be exploited to obtain fast computations. The smoother has to be an iterative regularization method. The grid transfer operator should preserve the regularization property of the smoother. This paper improves the iterative multigrid method proposed in [11] introducing a wavelet soft-thresholding denoising post-smoother. Such post-smoother avoids the noise amplification that is the cause of the semi-convergence of iterative regularization methods and reduces ringing effects. The resulting iterative multigrid regularization method stabilizes the iterations so that and imprecise (over) estimate of the stopping iteration does not have a deleterious effect on the computed solution. Numerical examples of signal and image deblurring problems confirm the effectiveness of the proposed method.

AMS subject classifications: 65F22, 65N55, 15B05

Key words: Multigrid methods, Toeplitz matrices, discrete ill-posed problems.

1. Introduction

Signal and image deblurring is an important task with many applications [18]. The blurring may be caused by object motion, calibration errors of the devices, or random fluctuations of the medium. We are concerning with restoration of blurred and noisy signals. The blurring process can be formulated in the form of Fredholm integral equations of the first kind. Let the function g represent the available observed blur- and noise-contaminated signal and let the function f represent the associated (unavailable) blur- and noise-free

*Corresponding author. *Email address:* `marco.donatelli@uninsubria.it` (M. Donatelli)

signal that we would like to recover. A first kind Fredholm integral equation for a one dimensional problem is as follows:

$$g(s) = \int_{\Omega} K(s,t) f(t) \mathrm{d}t, \qquad s \in \Omega, \tag{1.1}$$

where the point spread function (PSF) K is known. In our applications, K is smooth, the integral operator is compact and its inverse is unbounded if it exists. The task of solving (1.1) hence is an ill-posed problem [14]. In particular, we assume a spatially invariant PSF, that is, its effect depends only on the distance between s and t, thus, with a slight abuse of notation, we have

$$K(s,t) = K(s-t).$$

Discretization of (1.1) yields to a linear system of equations

$$A\mathbf{f} = \mathbf{g} = \mathbf{g}^{\text{blur}} + \mathbf{e}, \tag{1.2}$$

where A represents the blurring operator, $\mathbf{g}$ the available noise- and blur-contaminated signal, $\mathbf{g}^{\text{blur}}$ the blurred but noise free signal, and $\mathbf{e}$ the noise. The matrix A is a real Toeplitz matrix thanks to the space invariant property of the PSF. The ill-posedness of the continuous problem (1.1) implies that the matrix A is ill-conditioned and its singular values decay to zero without significant spectral gap, thus the linear system (1.2) is refereed as a discrete ill-posed problem [22]. This implies that straightforward solution of the linear system (1.2) does not provide a meaningful approximation of the desired signal because of the presence of the noise. A meaningful approximation of $\mathbf{f}$ can be determined by first replacing (1.2) with a nearby problem whose solution is less sensitive to perturbations in the data $\mathbf{g}$. This method is called regularization. Regularization methods include Tikhonov regularization or early termination of certain iterative methods [14]. Iterative methods provide an attractive alternative to Tikhonov regularization for large-scale problems [20]. When applied to ill-posed problems, many iterative methods exhibit a semiconvergence behavior. Specifically, the early iterations reconstruct information about the solution, while later iterations reconstruct information about the noise. The iteration number can be thought of as a discrete regularization parameter. A regularized solution is obtained by terminating the iterations after suitably few steps when the restoration error is minimized. Parameter selection methods such as discrepancy principle, GCV, and L-curve can be used to estimate the termination iteration [22]. The difficulty is that these techniques are not perfect and an imprecise estimate of the termination iteration can result in a solution whose relative error is significantly higher than the optimal, especially if the convergence is too fast and the restoration error curve is steep. Conjugate gradient type methods give reasonable results when applied to signal/image deblurring, but often they cut-off the high frequencies failing to recover the edges accurately.

Multigrid methods have already been considered to solve ill-posed problems [4, 5, 10, 21, 25, 26, 31]. They are usually applied to Tikhonov like regularization methods and no as iterative regularization methods. The first attempt in this direction was probably done in [11], where the authors combined an iterative regularization method used as pre-smoother with standard coarsening. A filter factor analysis of such multigrid method was done in [12]. A different multilevel strategy based on the cascadic approach was proposed in [30]. These multigrid methods have the main advantage to improve the regularization property of the smoother but this is also their main drawback. Indeed, the smoother fails to recover edges accurately and the same holds for these multigrid strategies. To overcome such problem nonlinear "corrections" were proposed in [15, 27]. The proposal in [15] combines the algorithm in [11] with an Haar wavelet decomposition and a non-linear residual correction step that preserves the edges. The proposal in [27] modifies the cascadic multilevel methods in [30] introducing nonlinear edge-preserving prolongation operators, which are defined via PDEs associated with total variation-type models.

This paper improves the iterative multigrid method proposed in [11] introducing a simple and computationally cheap denoising post-smoother. Both the residual correction in [15] and the nonlinear prolongation in [27] can be interpreted as a nonlinear post-smoother. Our post-smoother is the classical wavelet denoising by soft-thresholding proposed in [13]. The Toeplitz structure should be preserved at the coarser levels to obtain fast computations and a simple recursion. The full-weighting and the linear interpolation grid transfer operators correspond to linear B-spline [9] and preserve the Toeplitz structure at the coarse levels [2, 3]. Therefore, the denoising is done on a tight frame constructed from linear B-splines. The redundancy of tight frames is often useful in applications such as denoising, see, e.g., [7]. Our post-smoother performs only denoising without deblurring and so it avoids to add computationally expensive nonlinear deblurring methods, which could require to estimate regularizing parameters also at the coarse levels. In many applications we have a standard Gaussian white noise and a good enough estimation of the noise level is available. In such case, the threshold parameter for the wavelet denoising by soft-thresholding can be directly obtained from the noise level without further parameter estimations [13].

Our multigrid proposal combines an iterative regularization method (the pre-smoother) with a wavelet soft-thresholding denoising (the post-smoother) at different resolution scales, the refinement function is the symbol of the grid transfer operators of the multigrid method. Conjugate gradient-type methods performs deblurring and denoising in the Fourier domain, see, e.g., [20]. Therefore, our method regularizes both in the Fourier and the wavelet domain, with the same spirit of the ForWaRD method introduced in [28]. Moreover, our multigrid proposal falls in the recent idea to separate denoising from deblurring in an iterative way using two separate (efficient and existing) solvers, respectively, for denoising and deblurring [34]. The resulting method stabilizes the iteration so that an imprecise (over) estimate of the stopping iteration does not have a deleterious effect on the computed solution. Furthermore, the denoising post-smoother reduces the ringing effects and so it improves the restoration of the edges.

This paper is organized as follows. Section 2 describes multigrid methods for Toeplitz matrices and discusses some computational issues. Section 3 deals with the multigrid regularization method introduced in [11], while Section 4 concerns with a one level framelet denoising by soft-thresholding. Our iterative multigrid regularization method is described in Section 5. Numerical results in Section 6 illustrate the performance of the method. Section 7 discusses a 2D extension of our method with application to image deblurring problems. Finally, Section 8 summarizes conclusions and future work.

2. Multigrid methods for Toeplitz matrices

The matrix A in (1.2) is Toeplitz and square since the PSF is space invariant and we impose zero Dirichlet boundary conditions. More in detail, discretizing the integral equation (1.1) on a uniform grid and scaling by the discretization step, let a_j be the values of the function K at the grid points, for $j=-n+1,-n+2,\cdots,n-1$, the matrix A has the form

$$A=\begin{pmatrix} a_0 & a_{-1} & \cdots & \cdots & a_{-n+1} \\ a_1 & a_0 & a_{-1} & \cdots & a_{-n+2} \\ \vdots & \ddots & \ddots & \ddots & \vdots \\ \vdots & \ddots & \ddots & \ddots & a_{-1} \\ a_{n-1} & \cdots & \cdots & a_1 & a_0 \end{pmatrix}. \tag{2.1}$$

The entries a_j can be seen as the Fourier coefficients of a function z called symbol:

$$a_j=\frac{1}{2\pi}\int_{-\pi}^{\pi} z(x)\mathrm{e}^{-\mathrm{i}jx}\mathrm{d}x,$$

and the matrix A in (2.1) is denoted by $A=T_n(z)$. It is univocally identified by a vector of $2n-1$ elements and the matrix vector product can be computed in $O(n\log n)$ arithmetic operations by fast Fourier transforms, see, e.g., [19].

The original multigrid method for Toeplitz matrices was proposed by Fiorentino and Serra-Capizzano in [16] and was generalized by several other authors, see, e.g, [2,3,6,24]. Without loss of generality, we fix $n=2^\alpha-1$ for our convenience. We set $n_i=2^{\alpha-i}-1$, for $i=0,\cdots,m$, with $m<\alpha$. The prolongation is defined as

$$P_i=P_{n_i}(p_i)=T_{n_i}(p_i)K_{n_i}^T, \tag{2.2}$$

where $K_{n_i}\in\mathbb{R}^{n_{i+1}\times n_i}$ is the down-sampling matrix that picks up the entries with even index, for $i=0,\cdots,m-1$. Using the Galerkin approach, the restriction is P_i^T and the coarse matrices are $A_{i+1}=P_i^TA_iP_i$, for $i=0,\cdots,m$ and $A_0=A$.

We note that the matrix $A=T_n(z)$ in the linear system (1.2) has a symbol z that is a trigonometric polynomial because K has compact support, even if the number of nonzero diagonals of A can be large. We denote by $\mathbb{R}_q$ the set of trigonometric polynomials with degree up q, i.e., $z\in\mathbb{R}_q$ is such that $z(x)=\sum_{|j|\le q}a_j\mathrm{e}^{\mathrm{i}jx}$.

Remark 2.1. Let A_i be a Toeplitz matrix, then the matrix $A_{i+1}=P_i^TA_iP_i$, where P_i is defined in (2.2), is Toeplitz only if $p_i\in\mathbb{R}_1$, i.e., $T_{n_i}(p_i)$ is a tri-diagonal matrix.

The previous remark motivated the choice of the projectors in [3], the use of the Haar wavelets in [15], the impossibility to apply recursively the two-grid method in [6], and our tight frame in Section 4.

Proposition 2.1 ([3, 16]). *Let $A_i = T_{n_i}(z_i)$ with z_i a trigonometric polynomial and $P_i = P_{n_i}(p_i)$ defined in* (2.2) *with $p_i \in \mathbb{R}_1$. Then the matrix $A_{i+1} = P_i^T A_i P_i$ coincides with $T_{n^{(i+1)}}(z_{i+1})$, where*

$$z_{i+1}(x) = \frac{1}{2}\left(|p_i|^2 z_i\left(\frac{x}{2}\right) + |p_i|^2 z_i\left(\frac{x}{2}+\pi\right)\right). \tag{2.3}$$

The Fourier coefficients of z_i can be computed in $O(n_i)$ computing by convolution $|p_i|^2 z_i$ and than picking up a Fourier coefficient every two starting from the central coefficient of index zero, for $i = 1, \cdots, m$ and $z_0 = z$. They are usually computed just one time in a setup phase. If $z \in \mathbb{R}_q$, with $1 \ll q < n$ and $p_i \in \mathbb{R}_1$, the bandwidth of A_{i+1} is about one half of the bandwidth of A_i.

Proposition 2.2 ([1]). *Let $z_i \in \mathbb{R}_{q_i}$, $p_i \in \mathbb{R}_1$ and z_{i+1} defined in* (2.3)*. Then $z_{i+1} \in \mathbb{R}_{q_{i+1}}$ with $q_{i+1} \le \lfloor \frac{q_i}{2} \rfloor + 1$ and $q_{i+1} \le 2$ for i large enough (it depends on q).*

3. Multigrid regularization

The algebraic analysis of multigrid methods for Toeplitz positive definite matrices gives sufficient conditions on p_i and on the smoother to obtain a fast solver, see, e.g., [2, 3, 16]. In this paper the aim is different since we are concerning with regularization of discrete ill-posed problems.

A multigrid regularization method can be obtained combining an iterative regularization method, like some conjugate gradient-type methods, with a coarsening operator that projects the error equation in the subspace mainly formed by low and middle frequencies [11]. Grid transfer operators with such property are for instance the full-weighting and the linear interpolation, which symbol is

$$p(x) = \frac{1}{2}(1 + \cos(x)), \tag{3.1}$$

(up to a scaling factor). The mask of the Fourier coefficients of p is

$$h_0 = \frac{1}{4}[1\ 2\ 1], \tag{3.2}$$

see, e.g., [33]. Therefore, we fix $p_i = p$, for $i = 0, \cdots, m-1$.

Starting from an initial approximation $\mathbf{x} \in \mathbb{R}^n$ of (1.2), one two-level (TL) iteration provides a new approximation $\mathbf{y} \in \mathbb{R}^n$ according to:

$$\begin{array}{l} \mathbf{y} = \mathsf{TL}(\mathbf{x}, \mathbf{g}, \beta) \\ \hline \tilde{\mathbf{r}} = P_0^T(\mathbf{g} - A\mathbf{x}) \\ \tilde{\mathbf{y}} = \mathsf{Smooth}(\mathbf{0}, A_1, \tilde{\mathbf{r}}, \beta) \\ \mathbf{y} = \mathbf{x} + P_0\tilde{\mathbf{y}} \end{array} \tag{3.3}$$

where by $\mathsf{Smooth}(\mathbf{0}, A_1, \tilde{\mathbf{r}}, \beta)$ we denote the application of β steps of an iterative regularization method (smoother) to the linear system

$$A_1 \tilde{\mathbf{e}} = \tilde{\mathbf{r}} \tag{3.4}$$

with the null vector as initial guess.

The filter factor analysis in [12] shows that the two-level regularization strategy improves the regularization properties of the Landweber method when it is applied as smoother. Moreover, the TL algorithm saves some computational work with respect to the smoother because the iterative regularization is applied to the linear system (3.4) that has size $(n+1)/2-1$. On the other hand, it does not define a regularization method according to the definition in [14] because it does not compute the exact solution of the linear system (1.2) when the noise level goes to zero. A multilevel method can be easily obtained doing only few steps of the smoother (usually $\beta = 1$) and than applying recursively the algorithm.

Usually, the TL method (3.3) and its multilevel version provide oversmoothed restorations. This mainly depends on the smoother, classical iterative regularization methods (Landweber, CGLS, etc.) converge to the minimum norm least square solution of (1.2) and so compute oversmoothed restorations. To improve the restoration especially at the edges, in [15] a Haar wavelet projector is combined with a residual correction in the high frequencies. The disadvantage of this approach is that Haar wavelet computes blocky restorations and the residual correction step requires a nonlinear regularization with a parameter that should be estimated at each level. In the multilevel regularization method in [27] was applied a nonlinear prolongation, that we call post-smoother, that preserves the edges by a variational approach. In this paper, we take advantage from the multilevel strategy adding a soft-thresholding denoising in the high frequencies. In more details, at each level we apply a soft-thresholding denoising by framelets constructed from the linear B-spline (3.2).

4. Framelet denoising

In this section, we present some preliminaries of tight frame and denoising.

Let $\mathscr{A} \in \mathbb{R}^{k\times n}$ with $k \geq n$. The system, denoted by $\mathscr{A}$ again, consisting of all of the rows of $\mathscr{A}$ is a tight frame for $\mathbb{R}^n$ if for every $\mathbf{x} \in \mathbb{R}^n$ it holds

$$||\mathbf{x}||^2 = \sum_{\mathbf{y}\in\mathscr{A}} |\langle \mathbf{x}, \mathbf{y}\rangle|^2, \tag{4.1}$$

where $\langle\cdot,\cdot\rangle$ and $||\cdot|| = \langle\cdot,\cdot\rangle^{1/2}$ are the inner product and the norm of finite dimensional Euclidean spaces, respectively. Eq. (4.1) is equivalent to the perfect reconstruction formula

$$\mathbf{x} = \sum_{\mathbf{y}\in\mathscr{A}} |\langle \mathbf{x}, \mathbf{y}\rangle| \mathbf{y}.$$

The matrix $\mathscr{A}$ is called the analysis operator and its adjoint $\mathscr{A}^*$ is called the synthesis operator. The perfect reconstruction formula can be rewritten as $\mathbf{x} = \mathscr{A}^*\mathscr{A}\mathbf{x}$. Hence $\mathscr{A}$

DOI https://doi.org/10.4208/nmtma.2011.m12si03 | Generated on 2024-12-19 04:01:34

is a tight frame if and only if $\mathscr{A}^*\mathscr{A} = I$. We note that $\mathscr{A}\mathscr{A}^* \neq I$ in general, unless the system is orthogonal.

The tight frame $\mathscr{A}$ used in our algorithm is generated from the linear B-spline using the unitary extension principle [8]. Let p be defined in (3.1), as already noted, the trigonometric polynomial $\hat{h}_0 = p$ is the refinement symbol of the linear B-spline. The two corresponding high-pass filters (framelets)

$$\hat{h}_1 = \frac{\mathrm{i}}{\sqrt{2}}\sin(x) \quad \text{and} \quad \hat{h}_2 = \frac{1}{2}(1-\cos(x)),$$

$\mathrm{i}^2 = -1$, satisfy the condition of the unitary extension principle

$$\sum_{k=0}^{2} |\hat{h}_i(x)|^2 = 1 \quad \text{and} \quad \sum_{k=0}^{2} \overline{\hat{h}_i(x)}\hat{h}_i(x+\pi) = 0$$

for $x \in [-\pi, \pi]$. The corresponding masks are

$$h_0 = \frac{1}{4}[1,\ 2,\ 1], \quad h_1 = \frac{\sqrt{2}}{4}[1,\ 0,\ -1], \quad h_2 = \frac{1}{4}[-1,\ 2,\ -1].$$

In the following, we derive $\mathscr{A}$ from the masks associated with the previous framelet system. Imposing zero Dirichlet boundary conditions $\mathscr{A}^*\mathscr{A} \neq I$, thus we impose Neumann (symmetric) boundary conditions obtaining

$$H_0 = \frac{1}{4}\begin{bmatrix} 3 & 1 & 0 & \dots & 0 \\ 1 & 2 & 1 & & \\ & \ddots & \ddots & \ddots & \\ & & 1 & 2 & 1 \\ 0 & \dots & 0 & 1 & 3 \end{bmatrix}, \quad H_1 = \frac{1}{4}\begin{bmatrix} 1 & -1 & 0 & \dots & 0 \\ -1 & 2 & -1 & & \\ & \ddots & \ddots & \ddots & \\ & & -1 & 2 & -1 \\ 0 & \dots & 0 & -1 & 1 \end{bmatrix},$$

$$H_2 = \frac{1}{4}\begin{bmatrix} -1 & 1 & 0 & \dots & 0 \\ -1 & 0 & 1 & & \\ & \ddots & \ddots & \ddots & \\ & & -1 & 0 & 1 \\ 0 & \dots & 0 & -1 & 1 \end{bmatrix}.$$

In our algorithm we do not use a multilevel framelet system because the different resolution scales are already included in our multigrid algorithm, the grid transfer operator is the refinement mask (low-pass filter). Hence, we filter the noise only in the high frequencies of the current grid without apply a multilevel denoising and our analysis operator is

$$\mathscr{A} = \begin{bmatrix} H_0 \\ H_1 \\ H_2 \end{bmatrix}.$$

The denoising in the high frequencies is done by soft-thresholding. We fix the threshold parameter

$$\theta = c\sqrt{\frac{2\log(n)}{n}}, \tag{4.2}$$

for a constant $c > 0$. In the case of standard Gaussian white noise, the constant c can be chosen equal to the noise level if known. We use this value of c in the computed examples of Section 6. For $x \in \mathbb{R}$, we denote by $\mathrm{sgn}(x)$ the sign of x and by x_+ the positive part of x, i.e., $x_+ = x$ if $x > 0$ and $x_+ = 0$ if $x \leq 0$. The soft-thresholding applied to $\mathbf{d}$ is

$$\eta_\theta(\mathbf{d}) = \mathrm{sgn}(\mathbf{d})(|\mathbf{d}| - \theta)_+, \tag{4.3}$$

where the operations are intended componentwise.

In conclusion, the soft-thresholding denoising in the high frequencies is done by

$$\begin{array}{c} \mathbf{y} = \mathsf{Denoise}(\mathbf{x}, \theta) \\ \hline \begin{bmatrix} \mathbf{d}_0 \\ \mathbf{d}_1 \\ \mathbf{d}_2 \end{bmatrix} = \mathscr{A}\mathbf{x}, \qquad \begin{array}{l} \mathbf{c}_0 = \mathbf{d}_0 \\ \mathbf{c}_1 = \eta_\theta(\mathbf{d}_1) \\ \mathbf{c}_2 = \eta_\theta(\mathbf{d}_2) \end{array}, \quad \mathbf{y} = \mathscr{A}^* \begin{bmatrix} \mathbf{c}_0 \\ \mathbf{c}_1 \\ \mathbf{c}_2 \end{bmatrix}. \end{array} \tag{4.4}$$

5. The multigrid-framelet algorithm

In this section we modify the multigrid regularization method described in Section 3 adding the framelet denoising of Section 4 as post-smoother.

The multigrid regularization method in [11] does not apply the smoother at the finer level. In this way it is possible to reduce the computational cost and at the same time to increase the regularization property of the method. On the other hand, this implies that it is not possible to reconstruct the minimum norm least square solution of (1.2) when the noise level goes to zero. Therefore, in this paper we apply the pre-smoother also at the finer level, even if a detailed convergence analysis will be subject of future work. The method in [11] was introduced for image deblurring problems showing that a W-cycle iteration has about the same computational cost of the smoother applied at the finer level. Therefore in the following, we will use its W-cycle version and we will denote is as W-REG.

To keep our method as simple as possible, we apply the V-cycle with one step of pre-smoother, but other combination could be considered. The pre-smoother is an iterative regularization method like Landweber, CGLS, MR-II, etc. [20]. The post-smoother is not an iterative method but it is the framelet soft-thresholding denoising described in Section 4. The grid transfer operators P_i are defined in (2.2), where $p_i = p$ with p defined in (3.1) (standard coarsening), for $i = 0, \cdots, m-1$. From Proposition 2.2, the bandwidth of A_{i+1} is about one half the bandwidth of A_i and for i large enough it is equal to five since $p \in \mathbb{R}_1$. Therefore, the number of levels m can be fixed such that the coarse problem has size $n_m = 7$.

One iteration of our iterative multigrid regularization method is defined as follows

$$
\begin{array}{l}
\mathbf{y}_i = \mathsf{MGM}(i, \mathbf{x}_i, \mathbf{b}_i) \\
\hline
\texttt{If } (i = m) \texttt{ Then } \mathbf{y}_m = A_m^{-1}\mathbf{b}_m \\
\qquad\qquad\quad \texttt{Else } \tilde{\mathbf{x}}_i = \mathsf{Smooth}(\mathbf{x}_i, A_i, \mathbf{b}_i, 1) \\
\qquad\qquad\qquad\quad \mathbf{r}_{i+1} = P_i^T(\mathbf{b}_i - A_i\tilde{\mathbf{x}}_i) \\
\qquad\qquad\qquad\quad \mathbf{e}_{i+1} = \mathsf{MGM}(i+1, \mathbf{0}, \mathbf{r}_{i+1}) \\
\qquad\qquad\qquad\quad \hat{\mathbf{x}}_i = \tilde{\mathbf{x}}_i + P_i\mathbf{e}_{i+1} \\
\qquad\qquad\qquad\quad \mathbf{y}_i = \mathsf{Denoise}(\hat{\mathbf{x}}_i, \theta)
\end{array}
\tag{5.1}
$$

Given an initial guess $\mathbf{f}^{(0)} = \mathbf{0}$, the algorithm (5.1) generates the approximate solution

$$\mathbf{f}^{(k+1)} = \mathsf{MGM}(0, \mathbf{f}^{(k)}, \mathbf{g}).$$

The sequence of matrices $\{A_i\}_{i=0}^m$ is computed in a setup phase in $\mathcal{O}(n)$ arithmetic operations.

6. Numerical results

We present some numerical examples, which illustrate the regularization properties of our multigrid method (5.1). Comparisons with classical iterative regularization methods used as pre-smoother and with W-REG (the multigrid method in [11]) are reported. Different conjugate gradient-type methods are tested to show the flexibility of our proposal. The signal to be restored $\mathbf{f} \in \mathbb{R}^n$ has values in $[0, 1]$ and $n = 255$. The matrix A represents a Gaussian blurring operator with bandwidth equal to 59 and variance σ. The observed signal is obtained by adding a noise vector $\mathbf{e} \in \mathbb{R}^n$ to the blurred signal $\mathbf{g}^{\text{blur}} = A\mathbf{f}$. The noise vector has normally distributed entries with zero mean, scaled to yield a desired noise-level $\nu = \|\mathbf{e}\|/\|\mathbf{g}^{\text{blur}}\|$. We assume to know the noise level ν and we fix the thresholding parameter in (4.2) with $c = \nu$. A quantitative comparison of the restored signals is done computing the relative restoration error (RRE) $\|\hat{\mathbf{f}} - \mathbf{f}\|/\|\mathbf{f}\|$, where $\hat{\mathbf{f}}$ is the restored signal. The displayed restored signals provides also a qualitative comparison. All computations were performed with MATLAB 7.0.

We consider two examples with different features. In the first example the observed signal is slightly deteriorated, while in the second example it is affected by severe blur and noise. Fig. 1 shows the true signal $\mathbf{f}$ and the observed signal $\mathbf{g}$ for the two examples.

Example 1. The variance of the blur is $\sigma = 3$ and the noise level is $\nu = 1 \cdot 10^{-2}$.
Fig. 2 shows the RRE varying the number of iterations, for CGLS, for W-REG with CGLS as pre-smoother, and for our multigrid with CGLS as pre-smoother (MGM). In Fig. 2 we note the classical semi-convergence of CGLS with a minimum RRE at the iteration $k^* = 43$. Our multigrid method improves the regularization property of the smoother (CGLS) and stabilizes the iterations, i.e., it reduces the noise amplification that occurs at the iterations $k > k^*$. Indeed, the post-smoother denoising filters the noise amplified by the pre-smoother

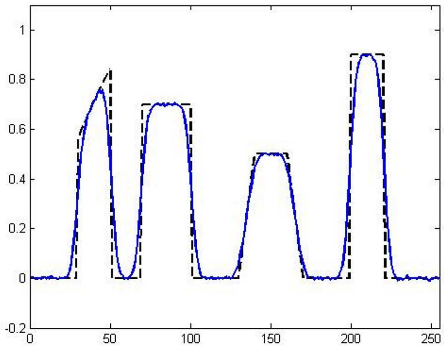

(a)

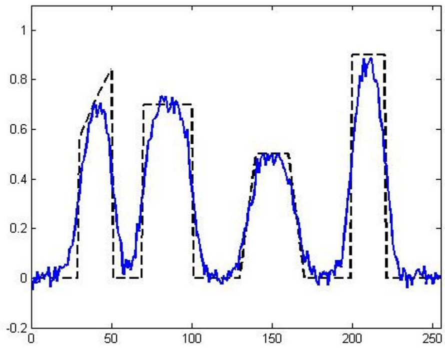

(b)

Figure 1: The dashed and solid curves depict the true and the observed signals, respectively. (a) Example 1 ($\sigma = 3$ and $\nu = 1 \cdot 10^{-2}$). (b) Example 2 ($\sigma = 5$ and $\nu = 6 \cdot 10^{-2}$).

for $k > k^*$. This leads to a less critical estimation of the stopping iteration, which could be over estimated without spoiling the restoration, especially if the pre-smoother has a very steep semi-convergence. W-REG stabilizes the iterations as well, but it is not able to reduce the ringing effects. Even if the RRE curve of our method remains flat for many iterations, a good restoration is computed also after few iterations. Fig. 3 shows the restored signals. Restored signals with our multigrid have lesser oscillations and a better restoration of the edges with respect to the restored signal with CGLS and W-REG. Visually the restorations obtained after 43 and 100 iterations of our method are about superposed (Fig. 3 (c) and (d)). Table 1 reports the RRE of the restored signals in Fig. 3.

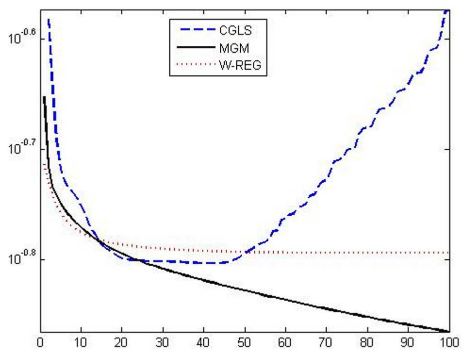

Figure 2: Example 1. The RRE versus the number of iteration: the dashed curve is CGLS, the dotted curve is W-REG, and the solid curve is MGM.

Example 2. The variance of the blur is $\sigma = 5$ and the noise level is $\nu = 6 \cdot 10^{-2}$. The matrix A is symmetric, thus we consider the MR-II instead of CGLS. Fig. 4 shows the RRE

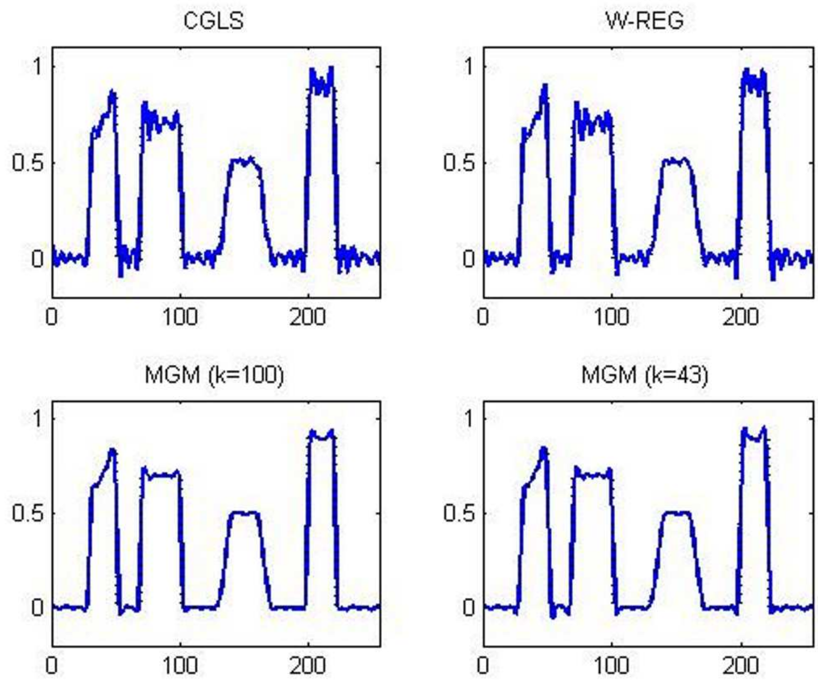

Figure 3: Example 1. Restored signals. The dotted curves depict the true signal.

Table 1: Example 1. RRE at the iteration k for CGLS, W-REG and MGM (the minimum RRE for CGLS is at the iteration $k^* = 43$ while for W-REG is at the iteration $k^* = 81$).

	$\|\|\mathbf{f}^{(\mathbf{k})} - \mathbf{f}\|\|/\|\|\mathbf{f}\|\|$	k
CGLS	0.157	43
W-REG	0.161	43
W-REG	0.160	81
MGM	0.151	43
MGM	0.136	100

varying the number of iterations for MR-II, for W-REG with MR-II as pre-smoother, and for our multigrid with MR-II as pre-smoother. In Figure 4 we note the classical semi-convergence of MR-II with a minimum RRE at the iteration $k^* = 8$. The convergence of W-REG is more stable with respect to MR-II. Our method has a lower and flatter RRE curve like in the previous example. The restored signal with our multigrid method has lesser ringing effects and a better restoration of the edges with respect to the other methods to MR-II also after few iterations when the RRE of the different methods is comparable (see Fig. 5 and Table 2). Indeed, Fig. 5 (b) shows that the restoration computed after 8 or 30 iterations of MGM method are comparable. Table 2 reports the RRE of the restored signals in Fig. 5.

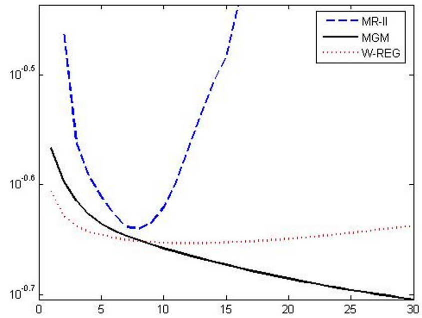

Figure 4: Example 2. The RRE versus the number of iteration: the dashed curve is MR-II, the dotted curve is W-REG, and the solid curve is MGM.

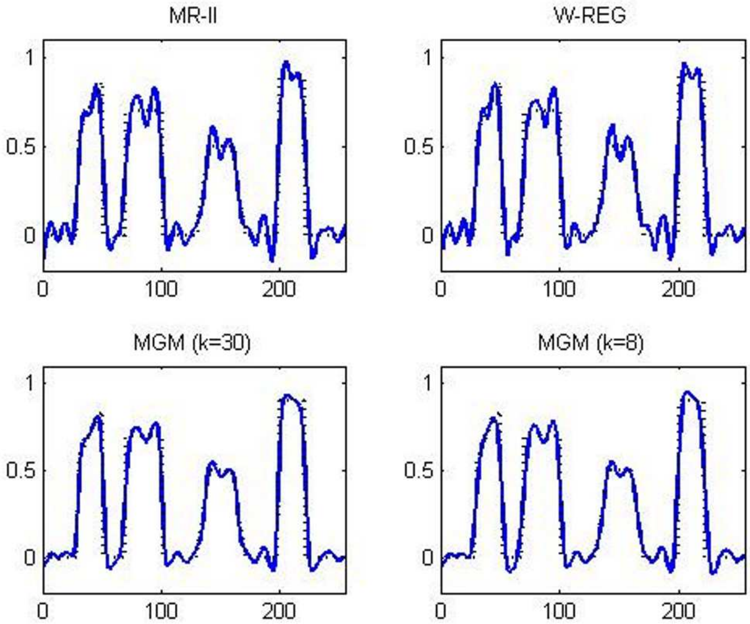

Figure 5: Example 2. Restored signals. The dotted curves depict the true signal.

Table 2: Example 2. RRE at the iteration k for MR-II, W-REG, and MGM (the minimum RRE for MR-II is at the iteration $k^* = 8$ while for W-REG is at the iteration $k^* = 12$).

	$\|\|\mathbf{f}^{(\mathbf{k})} - \mathbf{f}\|\|/\|\|\mathbf{f}\|\|$	k
MR-II	0.229	8
W-REG	0.224	8
W-REG	0.222	12
MGM	0.223	8
MGM	0.197	30

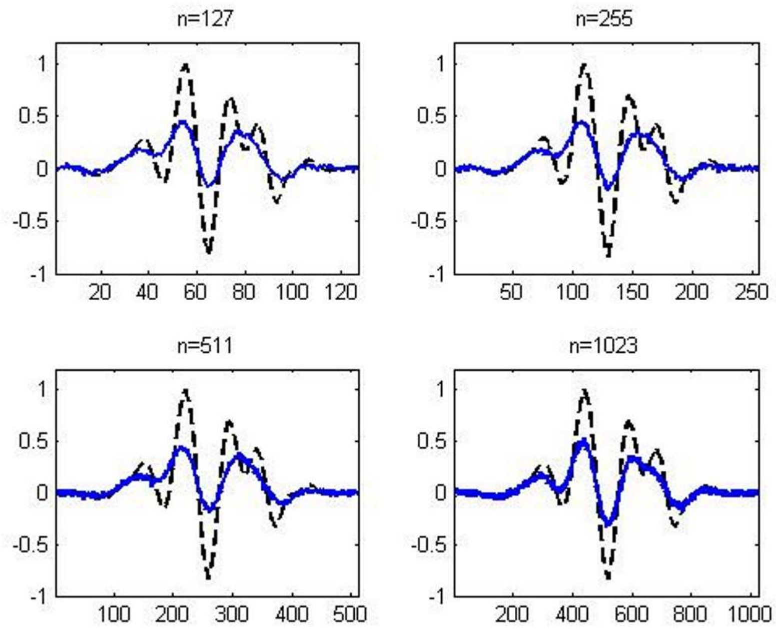

Figure 6: Example 3. The dashed and solid curves depict the true and the observed signals, respectively.

Table 3: Example 3. Minimum RRE with the number of the iteration where it is reached between brackets.

n	MR-II	W-REG	MGM
127	0.212 (8)	0.204 (2)	0.188 (7)
253	0.185 (9)	0.187 (2)	0.171 (13)
511	0.188 (10)	0.179 (1)	0.171 (13)
1023	0.128 (6)	0.085 (1)	0.092 (5)

Example 3. In this example, we consider a smooth signal without sharp edges and flat regions. Moreover, to show the scalability of our method, the same signal with a similar deterioration is restored at different scales, i.e., different sizes. Fig. 6 shows the true and the observed signals of size $n \in \{127, 255, 511, 1023\}$. Table 3 reports the minimum RRE for MR-II, W-REG and our MGM varying the size n of the signal. Between brackets is shown the iteration where the minimum RRE is reached. Fig. 7 and 8 show the restored signals for $n = 255$ and $n = 1023$ respectively. At all the different scales our method improves the restorations obtained with MR-II and W-REG with a flatter RRE curve like in the previous examples. Even if in this example there are not flat regions, we note that our method reduces the unnatural oscillations close to the boundary without smooth the high picks in the middle of the signal.

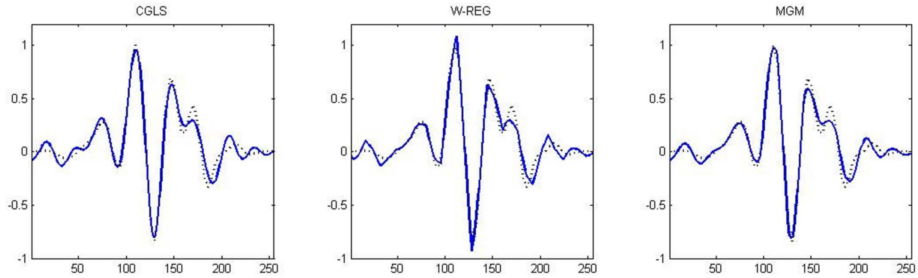

Figure 7: Example 3. Restored signals of size 255. The dotted curves depict the true signal.

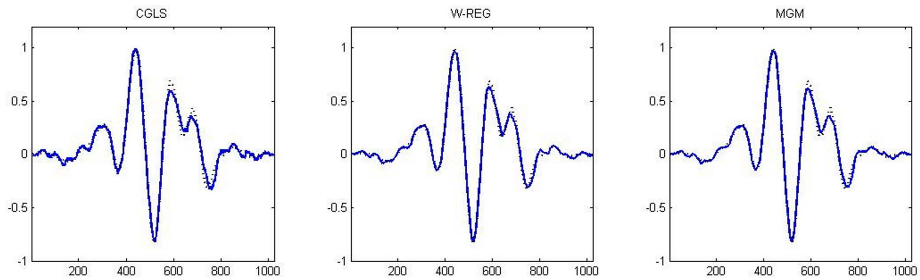

Figure 8: Example 3. Restored signals of size 1023. The dotted curves depict the true signal.

7. Image deblurring

In this section we propose a straightforward 2D extension of our algorithm. Let us consider the bidimensional version of the first kind Fredholm equation (1.1). Assuming a space invariant blur and imposing Dirichlet boundary conditions, the coefficient matrix of equation (1.2) is block Toeplitz with Toeplitz blocks, that is its entries a_j in (2.1) are Toeplitz matrices instead of scalar coefficients.

To define the denoising post-smoother, we construct 2D filters by tensor product of 1D filters. Let H_i, $i = 0, 1, 2$, be the linear B-spline filters defined in Section 4. We have nine 2D filters

$$H_{i,j} = H_i \otimes H_j, \qquad i, j = 0, 1, 2,$$

where $\otimes$ denotes the tensor product operator. $H_{0,0}$ is the only low-pass filter, while the others are high pass filters at least in one of the two directions. The analysis operator is

$$\mathscr{A} = \begin{bmatrix} H_{0,0} \\ H_{0,1} \\ \vdots \\ H_{2,2} \end{bmatrix}.$$

The denoising is obtained applying the soft-thresholding (4.3) to the high frequencies. The threshold parameter θ is chosen again according to (4.2). The algorithm (4.4) in 2D

Table 4: Examples 4-5. Minimum RRE with the number of the iteration where it is reached between brackets.

	Example 4	Example 5
CGLS	0.277 (15)	0.325 (11)
W-REG	0.277 (46)	0.325 (20)
MGM	0.267 (50)	0.315 (50)

becomes

$$\frac{\mathbf{y} = \mathsf{Denoise}(\mathbf{x},\theta)}{\begin{bmatrix} \mathbf{d_0} \\ \vdots \\ \mathbf{d_9} \end{bmatrix} = \mathscr{A}\mathbf{x}, \quad \begin{array}{l} \mathbf{c_0} = \mathbf{d_0} \\ \mathbf{c_i} = \eta_\theta(\mathbf{d_i}) \\ i = 2,\cdots,9 \end{array}, \quad \mathbf{y} = \mathscr{A}^* \begin{bmatrix} \mathbf{c_0} \\ \vdots \\ \mathbf{c_9} \end{bmatrix}.} \tag{7.1}$$

We consider a numerical example obtained from the Regularization Tools package by Hansen [23]. We call the function blur with the size $\mathsf{N} = 127$ and the bandwidth band $= 11$. We consider two examples with different blur and noise

Example 4: The variance of the blur is $\sigma = 2$ and the noise level is $\nu = 4 \cdot 10^{-2}$;

Example 5: The variance of the blur is $\sigma = 3$ and the noise level is $\nu = 9 \cdot 10^{-2}$.

Fig. 9 shows the true and the observed images of 127×127 pixels.

We use CGLS as pre-smoother and we stop the iterative methods when they reach the minimum RRE within fifty iterations. The results are reported in Table 4 and Fig. 10. Our MGM gives the best restoration and the flattest RRE curve. Fig. 11 and 12 show the restored image with the minimum RRE.

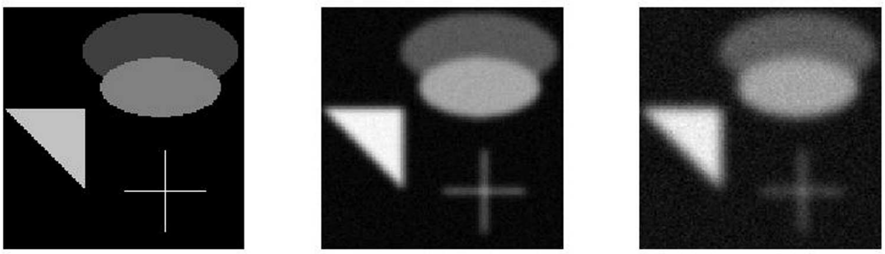

Figure 9: Examples 4-5. From left to right: true image, observed image of Example 4 ($\sigma = 2$ and $\nu = 4 \cdot 10^{-2}$), and observed image of Example 5 ($\sigma = 3$ and $\nu = 9 \cdot 10^{-2}$).

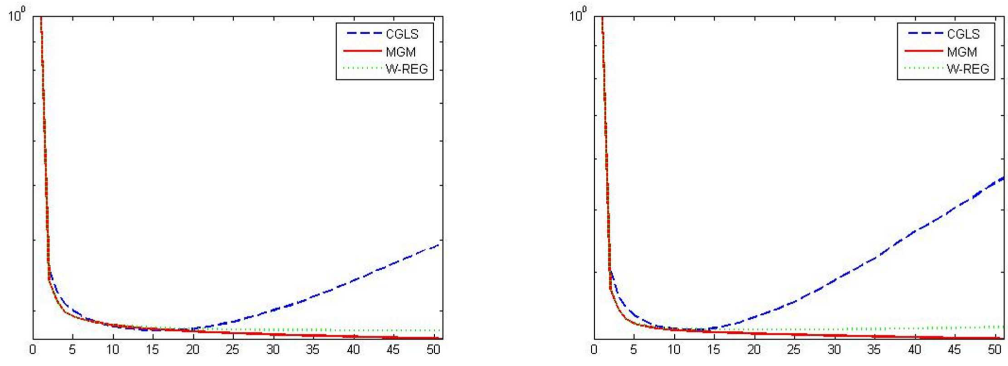

(a) (b)

Figure 10: The RRE versus the number of iteration: the dashed curve is CGLS, the dotted curve is W-REG, and the solid curve is MGM. (a) Example 1 ($\sigma = 2$ and $\nu = 4 \cdot 10^{-2}$). (b) Example 2 ($\sigma = 3$ and $\nu = 9 \cdot 10^{-2}$).

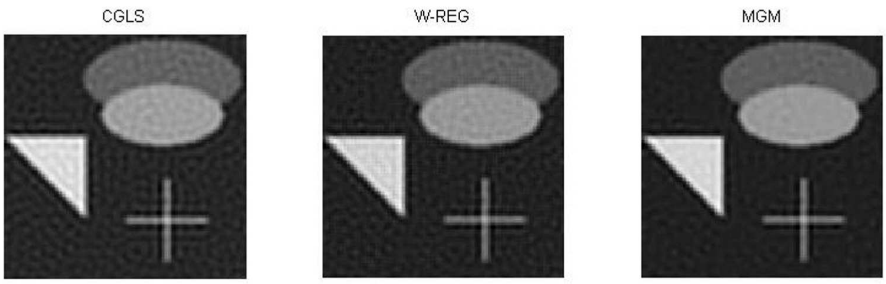

Figure 11: Example 4. Restored images.

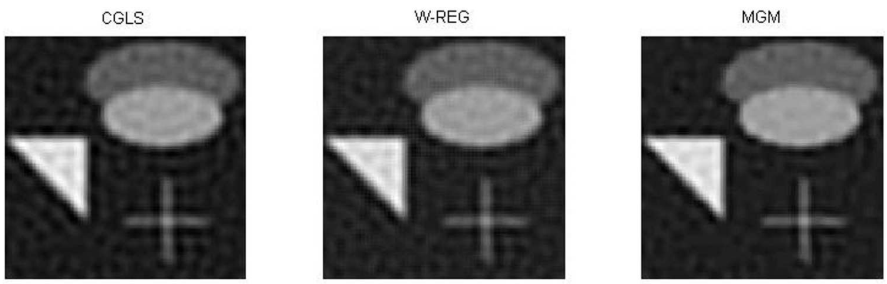

Figure 12: Example 5. Restored images.

8. Conclusions

In this paper, we have discussed some multilevel regularization methods with edge preserving strategies. We have proposed an improvement of the multigrid method in [11] adding a post-smoother framelet denoising by soft-thresholding, where the framelets are constructed from the refinable function of the grid transfer operator (linear B-spline). Our iterative multigrid regularization method for Toeplitz matrices combines a Fourier domain deconvolution (the pre-smoother iterative regularization method) with a wavelet domain denoising (the post-smoother soft-thresholding) by standard coarsening (a low-pass filter). The iterations are stabilized so that an imprecise (over) estimate of the stopping iteration does not have a deleterious effect on the computed solution. Moreover, the denoising post-smoother reduces the ringing effects and the noise amplification.

Further investigations are necessary, mainly to prove that our multigrid is a regularization method providing that it computes the minimal norm least square solution of (1.2) when the noise level go to zero. The multidimensional case and the estimation of the threshold parameter θ deserve a further study.

The future work could also consider other recent boundary conditions that lead to matrix algebras if the kernel K is symmetric [29, 32]. For such classes of matrices some fast multigrid solvers have already been developed [2] and they could be modified to obtain an iterative regularization method. The multigrid methods for matrix algebras preserve the same matrix structure also for high order grid transfer operators and hence wavelet/framelet decompositions of high orders (cubic for instance) could be used. Moreover, it could be investigated the use of iterative regularization methods for $L1$ regularization, like e.g. [17], as pre-smoother to improve the edge-preserving.

Acknowledgments This work was partly supported by MIUR (PRIN 2008 N. 20083KLJEZ).

References

[1] A. Aricò and M. Donatelli, *A V-cycle Multigrid for multilevel matrix algebras: proof of optimality*, Numer. Math., vol. 105, (2007), pp. 511–547.

[2] A. Aricò, M. Donatelli, and S. Serra Capizzano, *V-cycle optimal convergence for certain (multilevel) structured linear systems*, SIAM J. Matrix Anal. Appl., vol. 26, (2004) pp. 186–214.

[3] R. H. Chan, Q. Chang, and H. Sun, *Multigrid method for ill-conditioned symmetric Toeplitz systems*, SIAM J. Sci. Comput., vol. 19 (1998), pp. 516–529.

[4] R. H. Chan, T.F. Chan, and W. Wan, *Multigrid for differential-convolution problems arising from image processing*, in Scientific Computing, G. Golub, S.H. Lui, F. Luk, and R. Plemmons, eds., Springer-Verlag, Singapore, 1999, pp. 58–72.

[5] R. H. Chan and K. Chen, *A multilevel algorithm for simultaneously denoising and deblurring images* SIAM J. Sci. Comput., vol. 32, (2010), pp. 1043Ű1063,

[6] L. Cheng, H. Wang, and Z. Zhang, *The solution of ill-conditioned symmetric Toeplitz systems via two-grid and wavelet methods*, Comput. Math. Appl., vol. 46 (2003), 793-804.

[7] I. Daubechies, *Ten lectures on wavelets*, Society for Industrial and Applied Mathematics, Philadelphia, USA, 1992.

[8] I. Daubechies, B. Han, A. Ron, and Z. Shen, *Framelets: MRA-based constructions of wavelet frames*, Applied and Computational Harmonic Analysis, vol. 14 (2003), pp. 1–46.

[9] M. Donatelli, *An algebraic generalization of local Fourier analysis for grid transfer operators in multigrid based on Toeplitz matrices*, Numer. Linear Algebra Appl., vol. 17 (2010), pp. 179–197.

[10] M. Donatelli, *A Multigrid for image deblurring with Tikhonov regularization*, Numer. Linear Algebra Appl., vol. 12, (2005), pp. 715–729.

[11] M. Donatelli and S. Serra Capizzano, *On the regularizing power of multigrid-type algorithms*, SIAM J. Sci. Comput., vol. 27, (2006), pp. 2053–2076.

[12] M. Donatelli and S. Serra-Capizzano, *Filter factor analysis of an iterative multilevel regularizing method*, Electron. Trans. Numer. Anal., vol. 29 (2007/2008), pp. 163–177.

[13] D. L. Donoho, *De-Noising by Soft-Thresholding*, IEEE Trans. Inform. Theory, vol. 41, (1995), pp.613-627.

[14] H. W. Engl, M. Hanke, and A. Neubauer, *Regularization of Inverse Problems*, Kluwer Academic Publishers, Dordrecht, The Netherlands, 1996.

[15] M. I. Español and M. E. Kilmer, *Multilevel Approach For Signal Restoration Problems With Toeplitz Matrices*, SIAM J. Sci. Comput., vol. 32, (2010), pp. 299-319.

[16] G. Fiorentino and S. Serra-Capizzano, *Multigrid methods for Toeplitz matrices*, Calcolo, vol. 28 (1991), pp. 283–305.

[17] T. Goldstein and S. Osher, *The split Bregman method for $L1$-regularized problems*, SIAM J. Imaging Sci. vol. 2 (2009), pp. 323–343.

[18] R. Gonzalez and R. Woods, *Digital Image Processing*, Addison-Wesley, Reading, MA, 1992.

[19] U. Grenander and G. Szegö, *Toeplitz Forms and Their Applications*, Second Edition, Chelsea, New York, 1984.

[20] M. Hanke, *Conjugate Gradient Type Methods for Ill-Posed Problems*, Longman Scientific and Technical, Harlow, UK, 1995.

[21] M. Hanke and C. R. Vogel, *Two-Level Preconditioners for Regularized Inverse Problems I: Theory*, Numer. Math, vol. 83 (1998), pp. 385–402.

[22] P. C. Hansen, *Rank-Deficient and Discrete Ill-Posed Problems*, SIAM, Philadelphia, 1998.

[23] P. C. Hansen, *Regularization Tools Version 4.0 for Matlab 7.3*, Numer. Algo., vol. 46 (2007), pp. 189Ű194.

[24] T. Huckle and J. Staudacher, *Multigrid preconditioning and Toeplitz matrices*, Electron. Trans. Numer. Anal., vol. 13 (2002), pp. 81–105.

[25] B. Kaltenbacher, *On the regularizing properties of a full multigrid method for ill-posed problems*, Inverse Problems, vol. 17 (2001), pp. 767–788.

[26] J. T. King, *Multilevel algorithms for ill-posed problems*, Numer. Math., vol. 61 (1992), pp. 311–334.

[27] S. Morigi, L. Reichel, F. Sgallari, and A. Shyshkov, *Cascadic multiresolution methods for image deblurring*, SIAM J. Imaging Sci., vol. 1 (2008), pp. 51-74.

[28] R. Neelamani, H. Choi, and R. Baraniuk, *ForWaRD: Fourier-Wavelet Regularized Deconvolution for Ill-Conditioned Systems* IEEE Trans. Signal Process., vol. 52, (2004), pp. 418–433.

[29] M. Ng, R. H. Chan, and W. C. Tang, *A fast algorithm for deblurring models with Neumann boundary conditions*, SIAM J. Sci. Comput., vol. 21 (1999), pp. 851–866.

[30] L. Reichel and A. Shyshkov, *Cascadic multilevel methods for ill-posed problems*, J. Comput. Appl. Math., vol. 233 (2010), pp. 1314-1325.

[31] A. Rieder, *A wavelet multilevel method for ill-posed problems stabilized by Tikhonov regularization*, Numerische Mathematik, vol. 75 (1997), pp. 501–522.

[32] S. Serra Capizzano, *A note on anti-reflective boundary conditions and fast deblurring models*,

SIAM J. Sci. Comput. vol. 25, (2003) pp. 1307–1325.

[33] U. Trottenberg, C. W. Oosterlee and A. Schüller, *Multigrid*, Academic Press, 2001.

[34] Y. L. Wang, J. F. Yang, W. T. Yin, and Y. Zhang, *A new alternating minimization algorithm for total variation image reconstruction*, SIAM J. Imag. Sci., vol. 1 (2008), pp. 248–272.